

Supplementary information

Temperature-cycle Electron Paramagnetic Resonance

E. Gabriele Panarelli, Peter Gast and Edgar J.J. Groenen*

Department of Physics, Huygens-Kamerlingh Onnes Laboratory, Leiden University,
PO Box 9504, 2300 RA Leiden, The Netherlands

Calibration of the T-jump

Characterizing the temperature of the sample in the EPR cavity is possible thanks to the fact that solutions of nitroxide radicals show significant changes of their EPR spectrum as a function of temperature. Such changes are related to the rotational correlation time, τ_c , of the molecule in its medium. An expression of τ_c is given by Equation 1, which is the rotational-diffusion equivalent of the Stokes-Einstein equation, commonly used in EPR studies:

$$\tau_c = \frac{4\pi\eta r^3}{3k_B T} \quad (1)$$

with η and T being, respectively, the viscosity and the absolute temperature of the solution, r the hydrodynamic radius of the diffusing molecule, and k_B the Boltzmann constant.

Since τ_c is a function of the viscosity and of the temperature of the solution, the variations of the intensity and shape of the high-frequency EPR spectrum of nitroxide radicals represent a good indicator of the temperature changes of solutions whose viscosity varies strongly with temperature. In particular, mixtures of water and glycerol exhibit a strong dependence of their viscosity on temperature [1], and are thus particularly suited to be used as solvents of nitroxide radicals for a temperature calibration of a T-Cycle experiment. Following is a characterization of the temperatures reached upon application of T-jumps on a solution of TEMPOL in a mixture of water and glycerol.

Figure S1 shows the strong dependence on temperature (a) and on laser power (b) of the 275 GHz cw EPR spectrum of a TEMPOL solution (2 mM) in a mixture of water and glycerol 1:1 in volume.

A temperature calibration is possible by considering that to each temperature corresponds a unique value of the ratio of viscosity and temperature, η/T , of a solution of given composition. This is shown in Figure S2 (red dots), where tabulated values of η/T are plotted as a function of temperature, for a mixture of water and glycerol 60% in weight [1]. Since there is a unique relation between η/T and T , the same must be true for η/T and τ_c , as expressed by Equation 1. By simulating the spectrum at 23 °C of Figure S1(a) with EasySpin [2], a rotational correlation time $\tau_c = 100$ ps is found (in agreement with [3]). From this value and the viscosity of 7.75 cP obtained from [1], the hydrodynamic radius $r = 2.3$ Å follows from Equation 1, a value within the range reported in the literature [4]. With this value of r , it is possible to obtain ratios η/T from the EasySpin simulations of the spectra of Figure S1(a), and associate them to the corresponding temperatures. This is shown in Figure S2, where the blue dots (calculated from simulations) match quite well the red dots (tabulated). Note that the calculated points refer to a mixture of water and glycerol 50% in volume, which corresponds to 56% in weight, very close to the 60% weight composition of the tabulated data. In Figure S3 are shown the simulations run on the spectra of Figure S1(a).

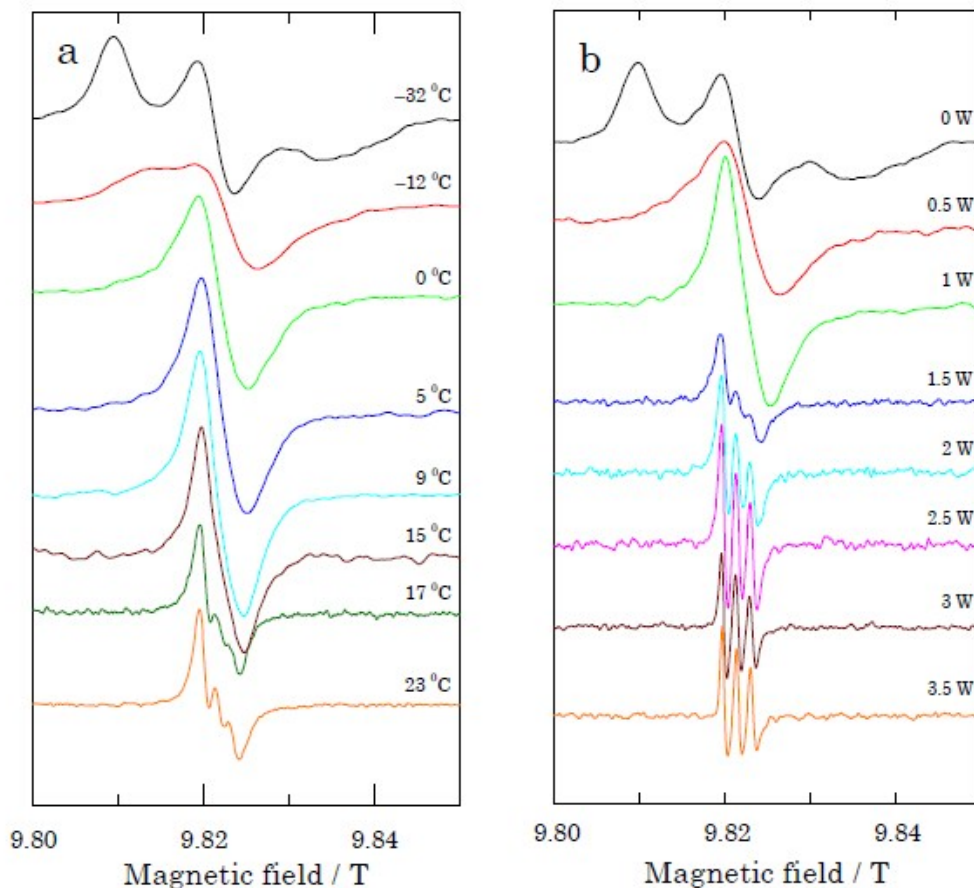


Fig. S1 (a) Temperature dependence of the 275 GHz cw EPR spectrum of a TEMPOL solution, at a concentration of 2 mM, in a mixture of water and glycerol 1:1 in volume. The temperature is changed with the cryostat settings. (b) The 275 GHz cw EPR spectrum of the same solution at a cryostat temperature of $-32\text{ }^{\circ}\text{C}$ under IR laser irradiation at different nominal powers.

Running EasySpin simulations on the spectra of Figure S1(b), as a function of nominal laser power, yields values of τ_c and, through Equation 1, ratios of η/T associated to each laser power. In Figure S4 are shown the simulations run on the spectra of Figure S1(b). By making use of the fit (red dotted line) of the tabulated points of Figure S2, it is possible to translate the ratios η/T into values of temperatures, and associate them to the respective nominal laser powers. Calculation of the relative T-jumps is then straightforward, and their relation to the laser power is shown in Figure S5, where a linear trend is observed within the evaluated errors (which is consistent with what is reported in [3] for T-jumps between 10 and 55 °C). T-jumps between roughly 20 to 120 °C have been obtained in the nominal power range

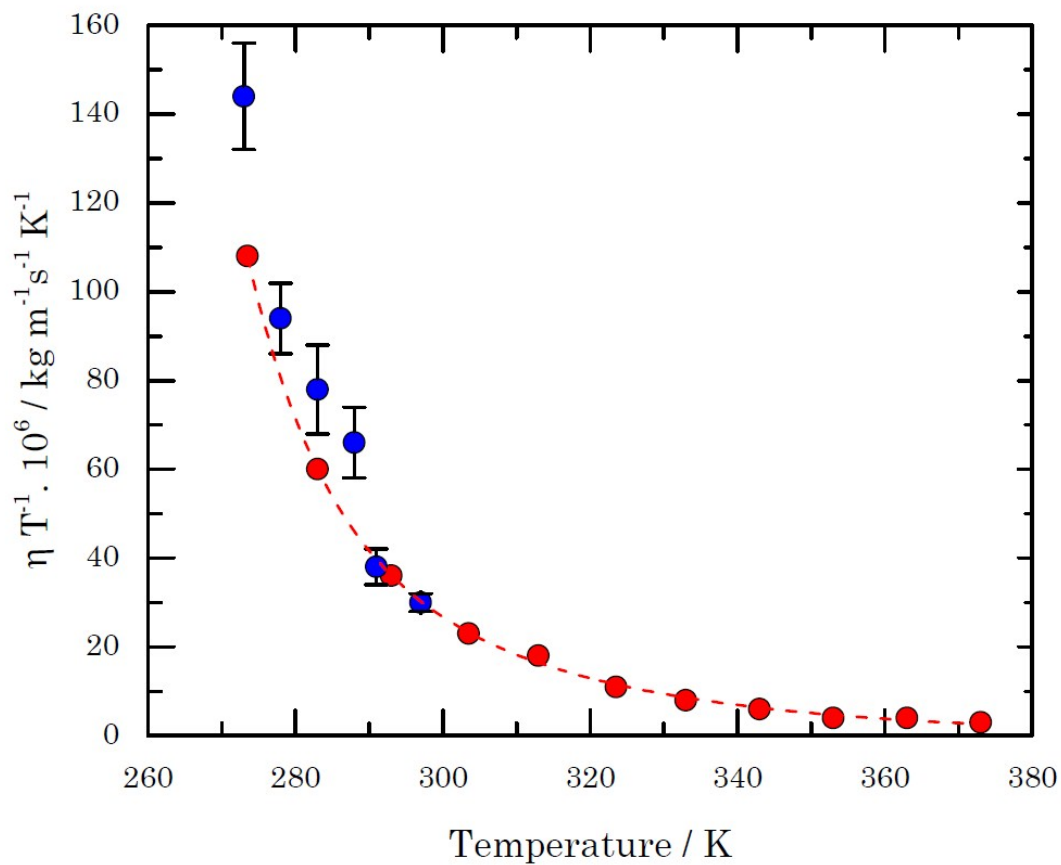


Fig. S2 Values of η/T plotted versus T . Red dots: obtained from [1] for a mixture of water and glycerol 60 % in weight. Blue dots: obtained with Equation [1] from the EasySpin simulations of the spectra of Fig. S1(a). The error bars are calculated from the error estimation on the τ_c calculated from the simulations.

between 0.5 to 3.5 W for the present laser setup (which differed from the one used for the T-cycle experiments reported in the main text). Notice that these values of T-jumps derive from the extrapolation of the experimental points of Figure S2 (blue dots) to higher temperatures, assuming they match the reference data points (red dots of Figure S2).

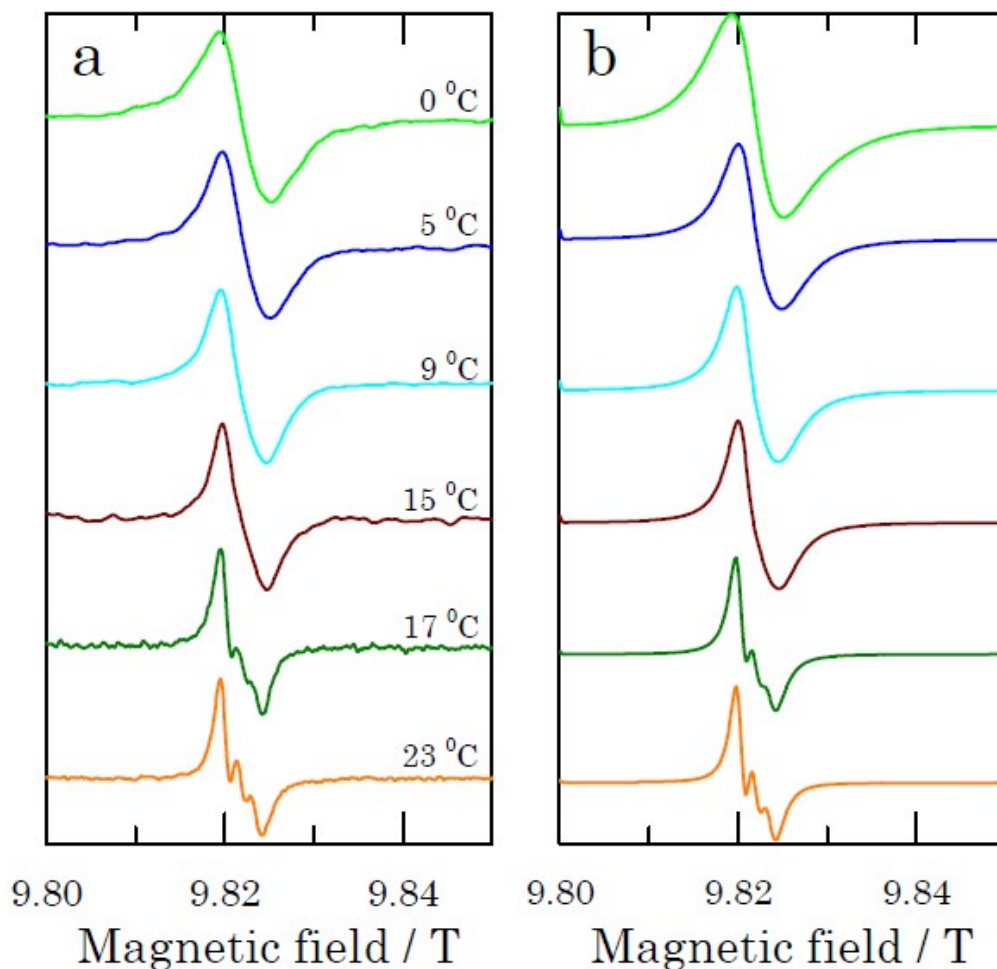


Fig. S3 EasySpin simulations (b) of the 275 GHz cw EPR spectra of TEMPOL as a function of temperature (a) from Fig. S1(a).

As a final remark, from Figure S1 it can be appreciated how the spectral linewidth decreases with increasing temperature or, equivalently, with increasing laser power. By defining what is here referred to as "partial linewidth", i.e., the full width at half maximum of the peak around 9.8195 T for the spectra of Figure S1(b), it is possible to obtain a measure of the line broadening of each spectrum. Notice that the partial linewidth can be unequivocally quantified only for the spectra that are not in the rigid-limit regime, in this case from 0 °C onwards. Since the partial linewidths are unambiguously associated to their corresponding laser powers, it is possible to link the T-jumps from Figure S5 - and therefore the temperature of the sample, taking into account the temperature of the cryostat - directly to the partial linewidths, as shown in Figure S6. Partial linewidths can thus be translated to temperatures in a one-to-one relation, which allows the determination of the latter in a convenient manner, since measuring the partial linewidth of the spectrum is a much easier and more straightforward procedure than obtaining rotational correlation times through simulations, or using the second-moment analysis described in [3].

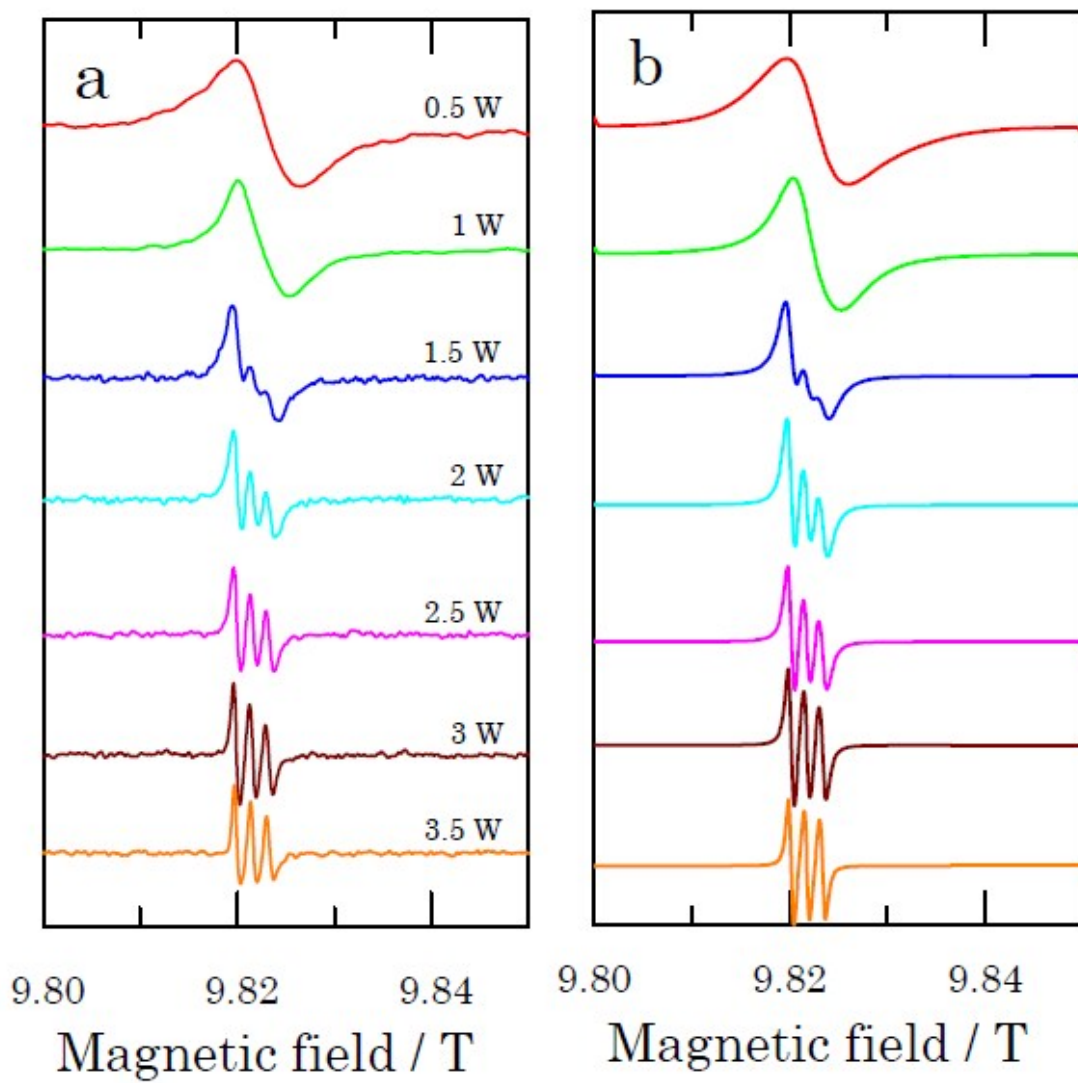


Fig. S4. EasySpin simulations (b) of the 275 GHz cw EPR spectra of TEMPOL as a function of laser power (a) from Fig. S1(b).

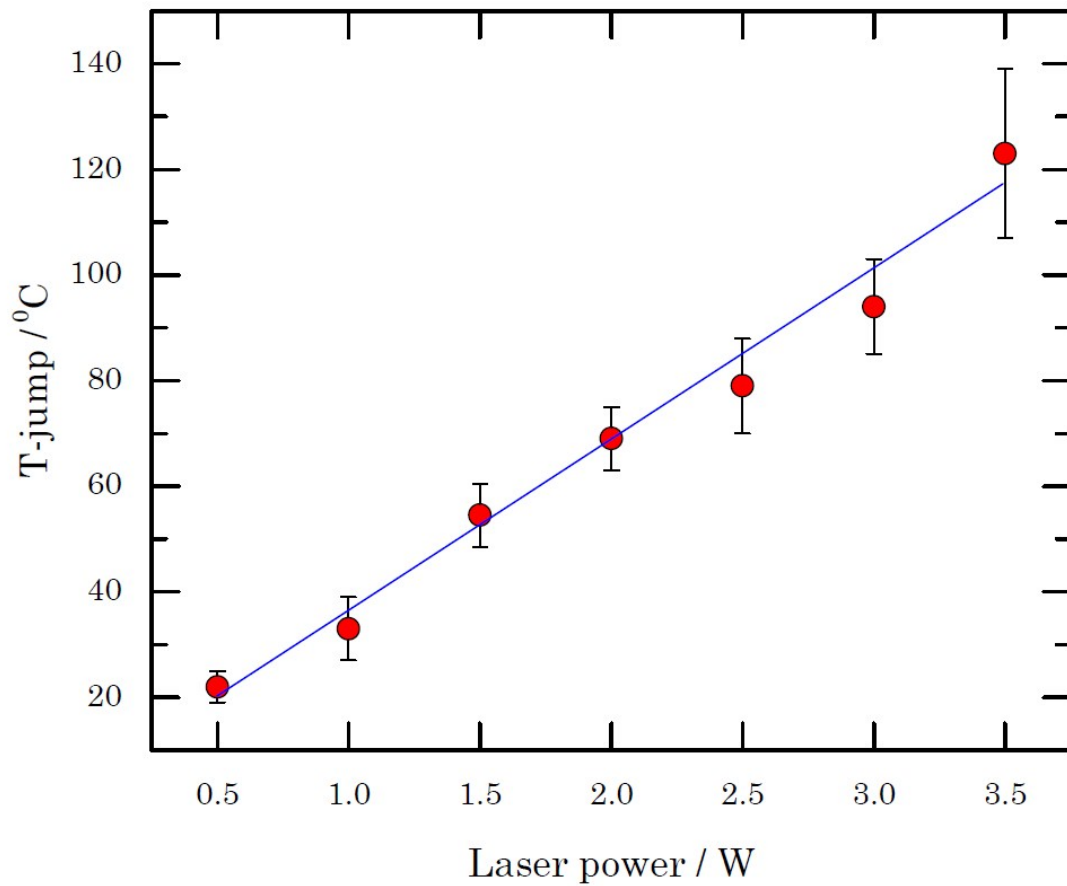


Fig. S5 T-jumps as a function of the nominal laser power. The T-jumps are calculated from the fitting of the values of T versus η/T (Fig. S2), from the starting temperature of -32 °C. The error bars are calculated from the error estimation on the τ_c calculated from the simulations.

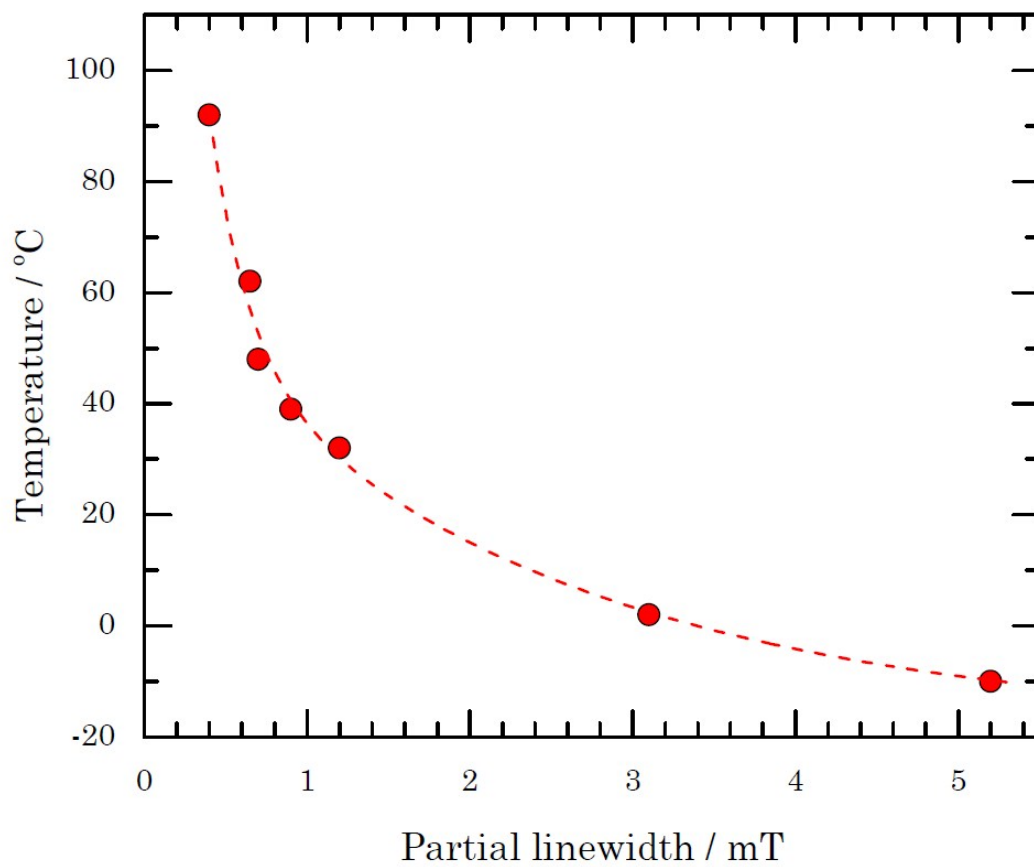


Fig. S6 Relation between the sample temperature and the partial linewidth of the corresponding 275 GHz cw EPR spectrum of TEMPOL in a mixture of water and glycerol 1:1 in volume. The dotted line is a guide to the eye.

Sub-zero mixing

A convenient feature of mixtures of water and glycerol is their low freezing point, which makes them highly viscous fluids at temperatures well below 0 °C [1]. Based on such property, a mixing method was devised, referred to as "sub-zero mixing", that allows an effective and simple hand mixing of the solutions of TEMPOL and sodium dithionite at a temperature of roughly -50 °C, i.e., a temperature at which the reaction is too slow to have an appreciable effect on the concentration of TEMPOL.

A 5-mL Pyrex beaker is kept inclined at about 45° and immersed in liquid nitrogen. A volume of 150 µL of one reagent is transferred into the inclined side of the beaker, as shown in Figure S7. Upon freezing of the solution, the beaker is inclined on the other side (while still being kept in liquid nitrogen), and a volume of 150 µL of the other reagent is transferred into that side, where it freezes. Care is taken to avoid the two solutions to ever be in physical contact. The beaker is then transferred into a polystyrene box partly filled with liquid nitrogen, and placed on a metal plate. By optimizing the level of liquid nitrogen in the polystyrene box and the flow of cold gaseous nitrogen blowing on the liquid nitrogen, the metal plate stabilizes at a temperature of about -60 °C, and the frozen solutions in the beaker warm up from liquid-nitrogen temperature to about -50 °C. At this temperature, the solutions have a toothpaste-like texture, and can easily be mixed with a pre-cooled spatula.

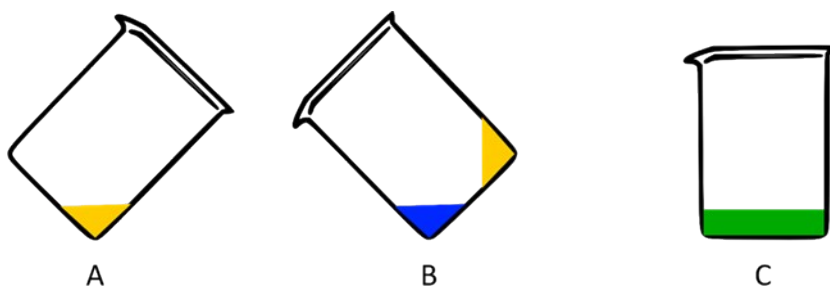


Fig. S7 Scheme of the steps for the sub-zero mixing. One reagent solution (depicted in yellow) is dropped on one side of the inclined beaker, where it freezes being at liquid nitrogen temperature (A). The other reagent solution (depicted in blue) is then dropped on the other side of the inclined beaker, and let to freeze (B). The beaker is finally placed on a metal plate, where it reaches a temperature of -50 °C, and it is possible to mix the two solutions (C).

Determination of the temperature of the sample during and immediately after the 250 ms laser pulse and a more detailed analysis of the reaction kinetics

In order to determine the temperature of the sample during and immediately after the laser pulse, we consider the change with temperature of the 275 GHz EPR spectrum of the same sample as used for the kinetic study, but without dithionite. This spectrum varies largely with temperature, as seen in Figure S8. In particular, the variation of the EPR intensity at 9.8182 T with temperature has been used to determine the course of the temperature of the sample during and immediately after the 250 ms laser pulse.

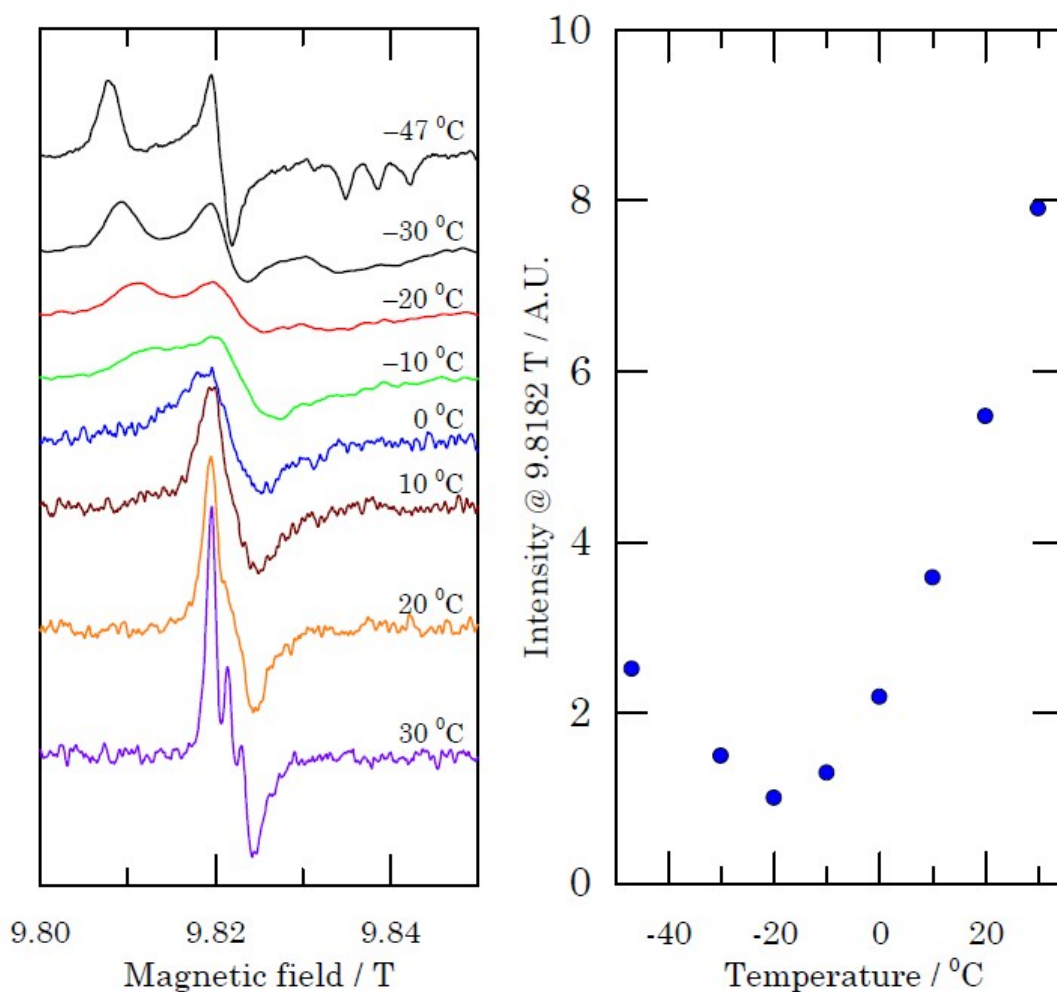


Fig. S8 Left: 275 GHz cw EPR spectrum as a function of the cryostat temperature of a 1 mM solution of TEMPOL in a mixture of glycerol and phosphate buffer (120 mM, pH 7.0), 1:1 in volume. Right: The corresponding intensities at the magnetic field of 9.8182 T as a function of temperature.

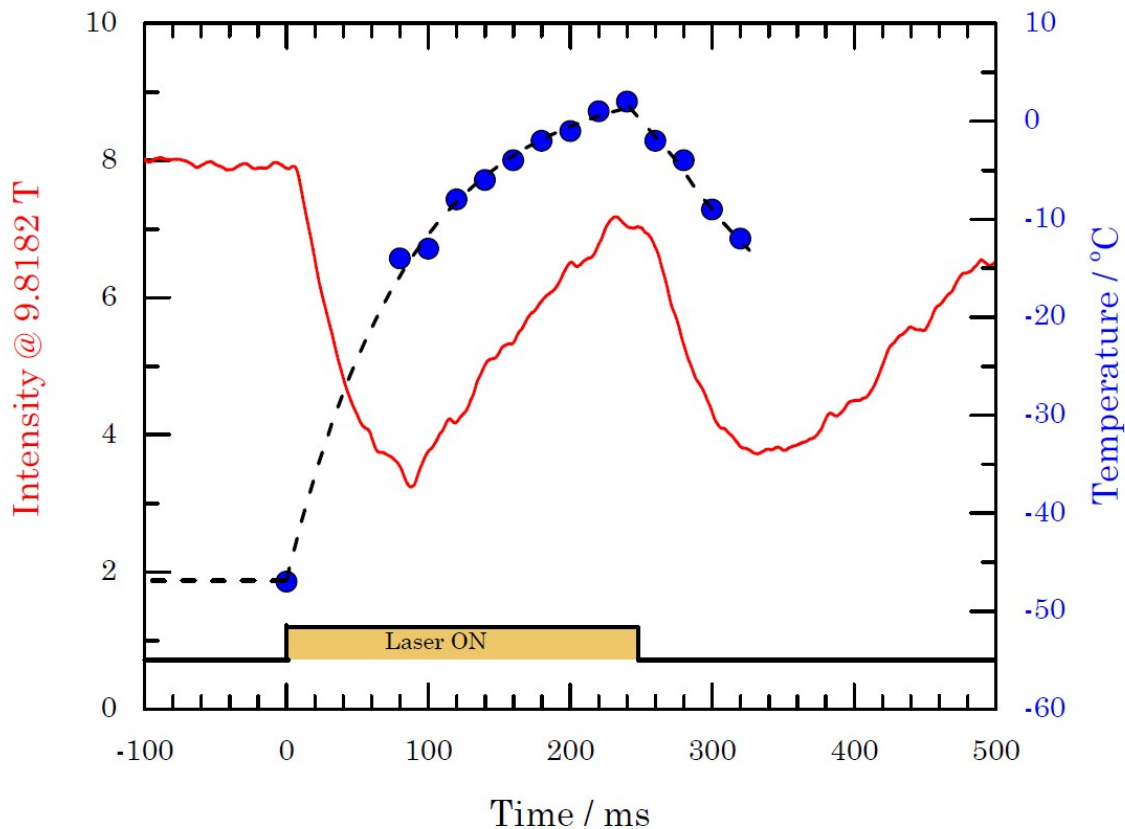


Fig. S9. Time profile (red line) of the 275 GHz EPR spectral intensity at the magnetic field of 9.8182 T of a 3 mM solution of TEMPOL in a mixture of glycerol and phosphate buffer (120 mM, pH 7.0), 1:1 in volume, before, during and after a laser pulse of 250 ms at 3.5 W. The intensity change is translated into a temperature change of the sample, as indicated by the blue dots (scale on the right). The dashed line serves as a guide to the eye.

The change of the 275 GHz EPR intensity of a solution of TEMPOL (3 mM, in a mixture 1:1 in volume of glycerol and phosphate buffer at 120 mM and pH 7.0) at the fixed magnetic field of 9.8182 T was measured while applying 250 ms long laser pulses at a nominal power of 3.5 W with a repetition time of 2 s. The time profile, shown in Figure S9, was obtained with a LeCroy WaveSurfer 424 oscilloscope. The signal was averaged 300 times, because of the high noise level caused by the spectrometer's time constant of 3 ms used to record the time profile. The TEMPOL solution was kept in the spectrometer's cryostat at a temperature of -47 °C. In this experiment, the EPR signal is monitored while the laser is switched on and off. In some cases, not for the one shown on Figure S9, small transient effects of detuning of the cavity were observed. These can be quantified and discriminated from the effects of the laser on the sample by measuring the EPR signal at a magnetic field outside the range of the EPR spectrum of the sample.

By comparing the time profile of the EPR intensity variation at 9.8182 T with the intensity variation at this magnetic field with temperature of Figure S8, the temperature change of the sample is obtained as represented by the blue dots in Figure S9. With a laser pulse of 250 ms the sample does not reach an equilibrium temperature, because the laser is switched off before an intensity plateau is attained. From the temperature of -47 °C at $t = 0$, before the laser pulse is applied, the sample reaches -8 °C at $t = 120$ ms, 2 °C at the end of the pulse, and is back at -8 °C at $t = 300$ ms. For the 250 ms pulse, the sample spends 180 ms at -3 ± 5 °C.

The variation in temperature of the sample during the 180 ms goes with a variation in the rate of the reaction. Indeed, the apparent rate constant $k' = 1.8 \pm 0.2 \text{ s}^{-1}$ reported in the manuscript represents an average value. This average value, say $\langle k' \rangle$, can be modeled as follows. Firstly, the time interval $\Delta t = 180 \text{ ms}$ that the sample spends at a temperature higher than or equal to $-8 \text{ }^\circ\text{C}$ is divided into n time elements δt , for whose length the temperature of the sample, and therefore the rate constant, can be considered constant. The decay of the 275 GHz EPR intensity of TEMPOL during the time interval Δt can be expressed as

$$I = I_0 e^{-\langle k' \rangle \Delta t} \quad (2)$$

where $\Delta t = n\delta t$ and the average apparent rate constant is defined as $\langle k' \rangle = \frac{1}{n} \sum_{i=1}^n k'_i$. Secondly, knowing $k'(-28^\circ\text{C}) = 0.063 \text{ s}^{-1}$, and assuming an initial value of $k'(19^\circ\text{C})$, it is possible to calculate $k'(T)$ at the intermediate temperatures defined by the time elements δt (cf. Figure S9), and thus $\langle k' \rangle$, assuming the $k'(T)$'s behave according to the Arrhenius equation. For a time step $\delta t = 1 \text{ ms}$, the temperature (and thus k') can be considered constant during this time. In an iterative manner, the value of $k'(19^\circ\text{C})$ is varied until the experimental average rate $\langle k' \rangle = 1.8 \text{ s}^{-1}$ is reproduced. In this way, the value of $k'(19^\circ\text{C}) = 18 \pm 2 \text{ s}^{-1}$ is obtained, which, with a sodium dithionite concentration of 50 mM, yields $k(19^\circ\text{C}) = 360 \pm 50 \text{ M}^{-1}\text{s}^{-1}$. In addition, the activation energy is found equal to $70 \pm 4 \text{ kJ mol}^{-1}$.

Modeling of the temperature decay following a laser pulse.

In order to investigate whether reducing the size of the sample volume and/or increasing the ΔT of the T-jump may accelerate the cooling process, model calculations of the heat transfer were performed using the COMSOL Multiphysics software (version 5.3 a). To model the experimental conditions, a simplified geometry of an ensemble of five cylinders was created.

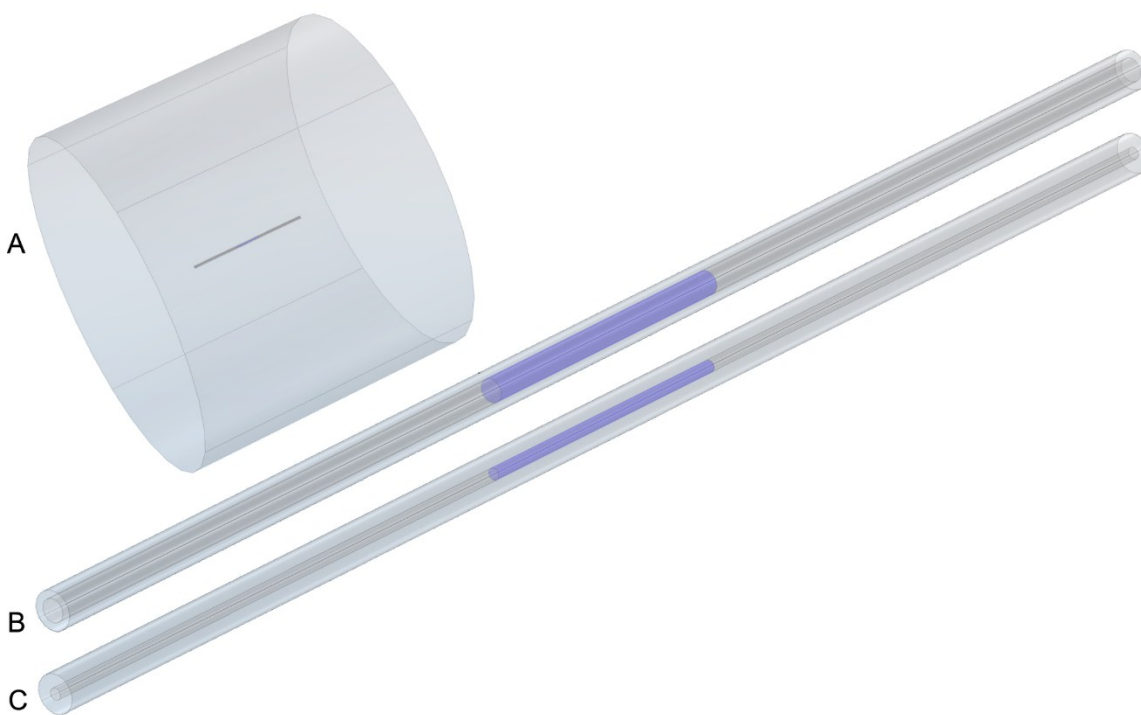


Fig. S10. Geometry of the model used to calculate the temperature profiles of Figure S11 with the COMSOL Multiphysics software. (A) Cylinder of helium (diameter 30 mm, length 25 mm), having the sample in its center, shown enlarged in (B) and (C). (B) Quartz capillary (total diameter 250 μm , thickness 50 μm , length 10 mm) with water and glycerol 1:1 in volume as the sample, highlighted in purple (diameter 150 μm , length 2 mm). (C) Same as (B), but the quartz capillary thickness is 87.5 μm , so that the sample diameter is 75 μm .

- A cylinder made of helium, much bigger than the sample size, acting as a thermal bath that simulates the cryostat;
- A much smaller cylinder made of quartz, placed in the center of the helium cylinder, representing the portion of the capillary used as a sample holder for 275 GHz experiments that is located in the spectrometer's cavity, and in the proximity thereof;
- A cylinder made of a mixture of water and glycerol 1:1 in volume, put inside the quartz cylinder, and representing the sample;
- Two cylinders made of helium gas, placed inside the quartz cylinder and at the two sides of the sample cylinder, used as a filling to avoid the quartz cylinder to be a solid quartz block.

The temperature at time $t = 0$ of all the cylinders was set to either 243 K or 223 K, except for the sample cylinder whose temperature was set to 303 K.

Two major simplifications were made in the model, with the purpose of reducing the complexity of the system and saving computational time. First, no active cooling of the bath was taken into account, but rather a large volume of helium gas was created, containing the sample (of much smaller volume) at its center; refer to Figure S10 for the geometry used in the simulations. The volume of the helium gas used as a thermal bath (~ 20 mL), much larger than that of the sample (~ 35 nL), ensures that the temperature of the bath is maintained at 243 K (or 223 K), as the sample cools down from the initial temperature of 303 K. The second simplification regards the initial temperature of the quartz containing the sample, and the helium gas inside the quartz, on both sides of the sample: in the simulations their temperature at $t = 0$ was set equal to that of the outer helium bath; nonetheless, more realistically a temperature gradient is present through the walls of the quartz capillary, and along the helium gas directly in contact with the sample. However physically inaccurate these two simplifications might be, in consideration of the degree of accuracy needed for the present study, they actually represent a minor deviation from the physical processes of interest here, and they allow a beneficially shorter calculation time.

As far as the meshing is concerned, since the interesting temperature variations to simulate were those of the sample, the size of the meshing patterns were set differently for the sample cylinder ("Extremely Fine" mesh) as compared to the other cylinders ("Fine" mesh for the quartz cylinder, "Coarse" or "Normal" mesh for the helium cylinders inside the quartz, and "Extremely Coarse" mesh for the bigger helium cylinder). In all cases, the meshes were automatically generated with the program's "physics-controlled" algorithm. The physical properties as a function of temperature needed to perform the simulations (i.e., heat capacity at constant pressure, density, thermal conductivity, and dynamic viscosity) were taken automatically from the COMSOL Multiphysics library for quartz and helium; the properties of the mixture of water and glycerol 1:1 in volume had to be specified manually and were obtained from [1].

Figure S11 shows the output of four different simulations, the sample diameter being either 150 or 75 μm (A, C and B, D respectively), and the temperature of the bath being either 243 K or 223 K, thus the ΔT being either 60 K or 80 K (A, B and C, D respectively). The sample's temperature decay from the initial value of 303 K is calculated for each mesh point of the sample cylinder; since both the surface points and the inner points are evaluated, and the former are subject to a faster cooling than the latter, the result is a temperature decay represented as a band in the plots of Figure S11. When comparing plot A with B, and C with D, a shortening of the cooling time is observed, as a result of a four-fold decrease of the sample volume. Similarly, when comparing plot A with C, and B with D, a shortening of the cooling time is observed resulting from an increase of the ΔT between the sample and the bath. To better illustrate these temperature decays quantitatively, Table 1 summarizes the average time it takes, in each case, for the sample cylinder to reach the temperature of 270 K from 303 K. The most dramatic effect can be appreciated when the sample diameter is reduced by half: for both ΔT considered, the cooling time becomes about five times shorter. Also changing the ΔT from 60 to 80 K reduces the cooling time significantly (of about two times), for both sample diameters considered.

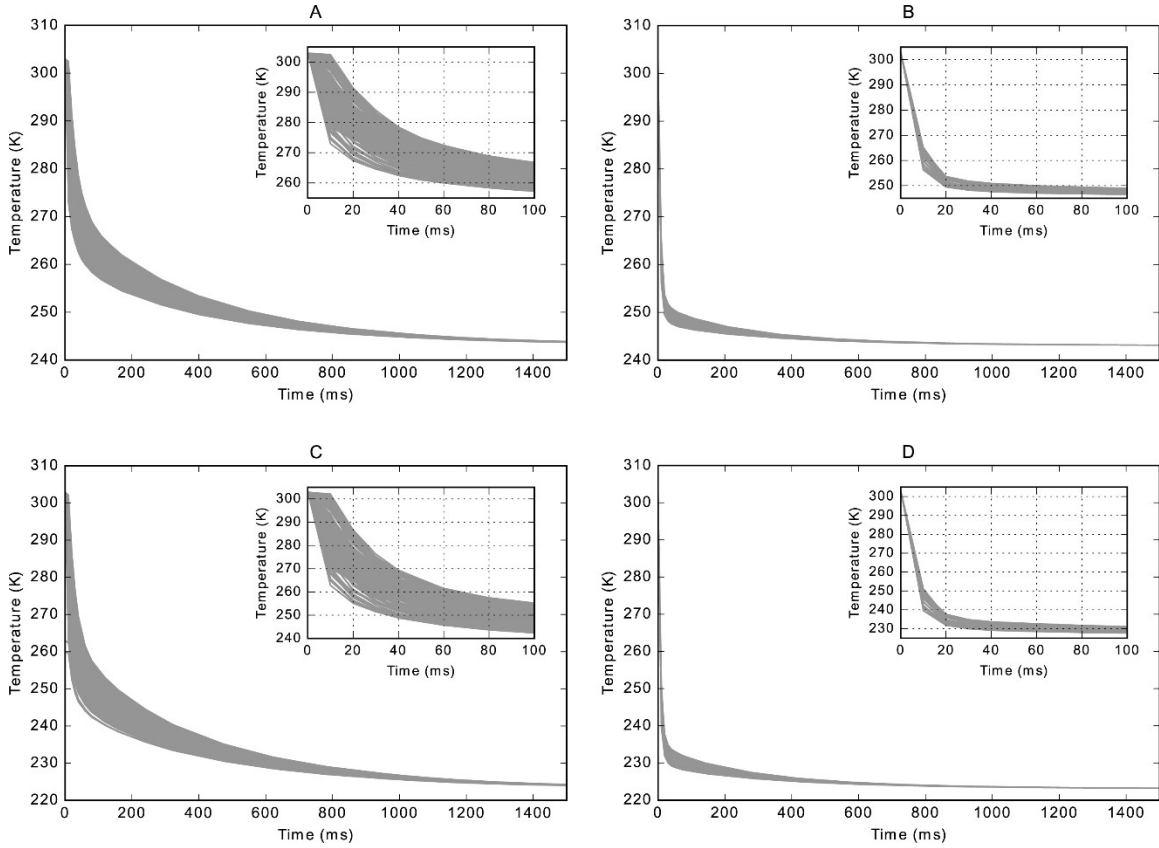


Fig. S11. Temperature decays as a function of time, simulated with the COMSOL Multiphysics software. Each gray band is made of lines each representing the temperature decay at a specific spatial coordinate of the sample cylinder, so that the whole volume of it (i.e., the surface points as well as the inner points) is taken into account. The graphs show the decay of the sample cylinder from a temperature of 303 K, with the bath at a starting temperature of 243 K (plots A and B) or 223 K (plots C and D). The diameter of the sample cylinder is 150 μm (plots A and C) or 75 μm (plots B and D). In each plot, the inset shows the decay in the first 100 ms.

ΔT	$d = 150 \mu\text{m}$	$d = 75 \mu\text{m}$
60 K	$\langle t_A \rangle = 44 \text{ ms}$	$\langle t_B \rangle = 8 \text{ ms}$
80 K	$\langle t_C \rangle = 23 \text{ ms}$	$\langle t_D \rangle = 5 \text{ ms}$

Table 1. Variations of the average time $\langle t \rangle$ it takes the sample to reach the temperature of 270 K starting from 303 K, by changing two parameters in the simulations: the diameter d of the sample cylinder, and the temperature difference ΔT between the sample and the bath. The subscripts A, B, C, and D refer to the plots of Fig. S11, where the $\langle t \rangle$'s are taken from.

From the simulations it thus appears that it is possible to improve the current implementation of the T-Cycle technique as far as the time for the cooling of the sample is concerned, at least by acting on two factors. One is the reduction of the sample volume, and therefore the increase of the thickness of the capillary walls; this, however, comes at the cost of a smaller signal, which might constitute a problem for low-concentrated samples. Moreover, reducing the sample diameter implies having a shorter optical path for the laser absorption, which might result in a less efficient laser-induced heating, as the sample's absorbance scales with the path length according to the Lambert-Beer law. The other factor is the increase of the ΔT between the sample and the bath, or, in other words, the increase of the T-jump. Both factors contribute to a significant reduction of the cooling time of the sample, which thus in principle enables a better time resolution.

References

- [1] Physical Properties of Glycerine and its Solutions . Glycerine Producers' Association, New York, 1963.
- [2] S. Stoll, A. Schweiger, EasySpin: a comprehensive software package for spectral simulation and analysis in EPR, *Journal of Magnetic Resonance*, 2006, **178**, 42-55.
- [3] M. Azarkh, E.J.J. Groenen, Temperature determination by EPR at 275 GHz and the detection of temperature jumps in aqueous samples, *Journal of Physical Chemistry B*, 2015, **119**, 13416-13421.
- [4] N.A. Chumakova, V.I. Pergushov, A.K. Vorobiev, A.I. Kokorin, Rotational and translational mobility of nitroxide spin probes in ionic liquids and molecular solvents, *Applied Magnetic Resonance*, 2010, **39**, 409-421.